

Supplementary Materials: Visualization of Fluoride Ion In Vivo Using a Gadolinium(III)-Coumarin Complex-Based Fluorescence/MRI Dual-Modal Probe

Yue Wang, Renfeng Song, Huan Feng, Ke Guo, Qingtao Meng, Haijun Chi, Run Zhang and Zhiqiang Zhang

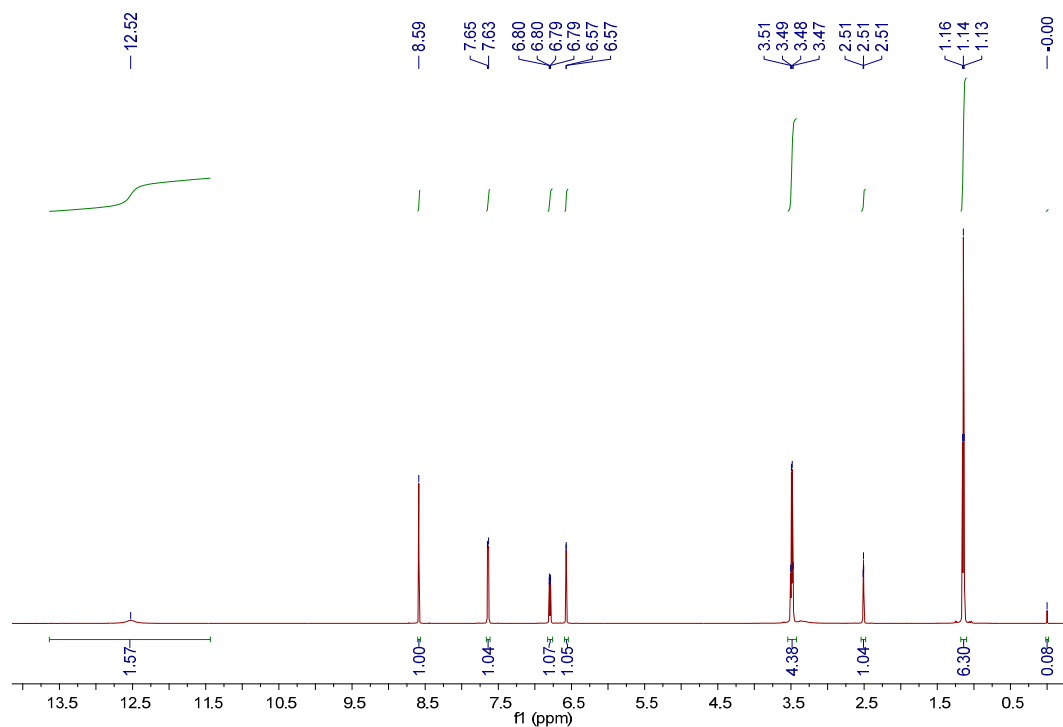


Figure S1. ¹H-NMR of CA (DMSO-*d*₆).

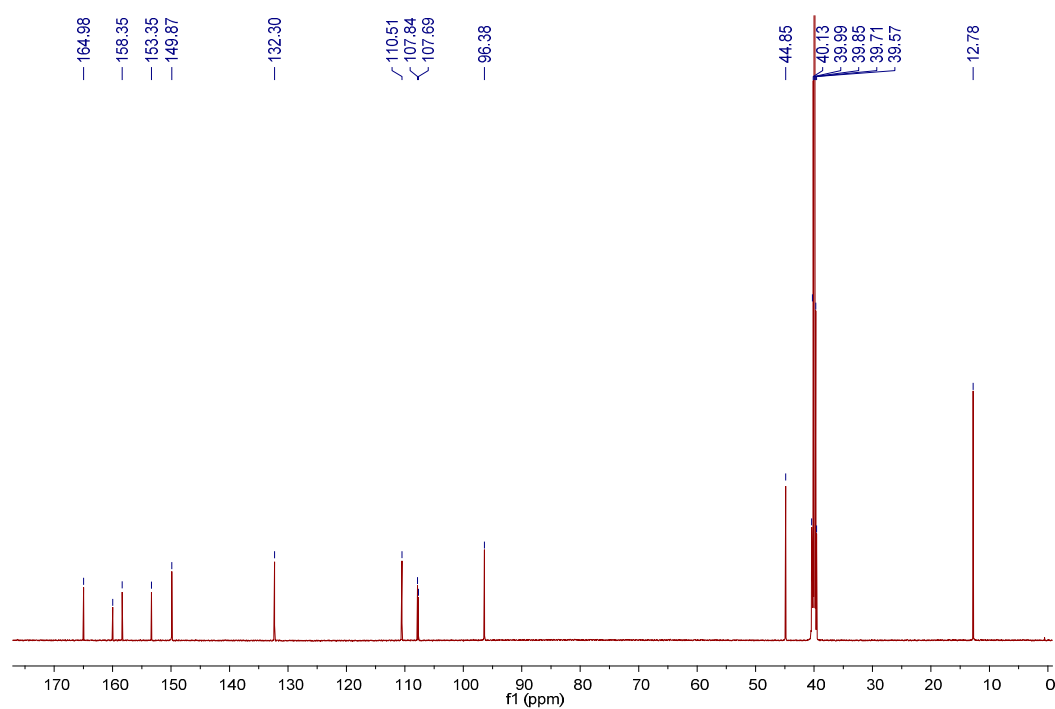


Figure S2. ¹³C-NMR of CA (DMSO-*d*₆).

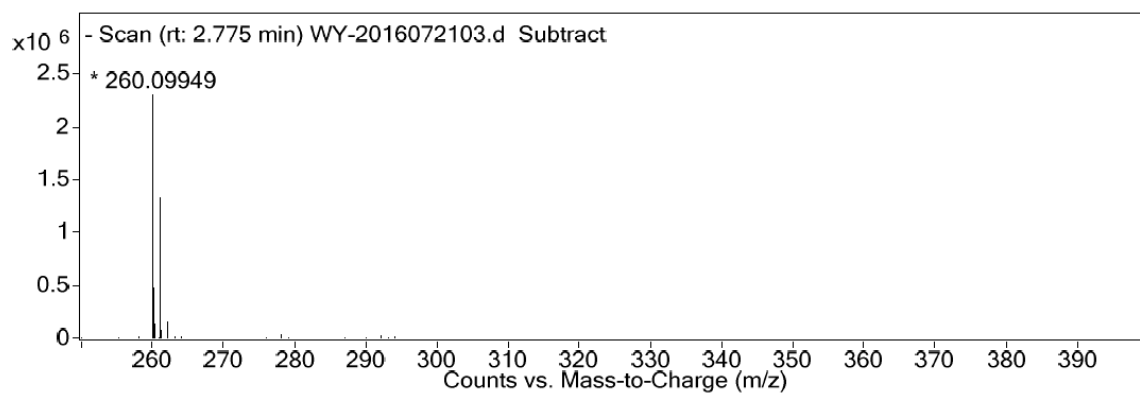


Figure S3. High resolution MS spectrum of 4-(diethylamino)-coumarin-3-carboxylic acid (CA).

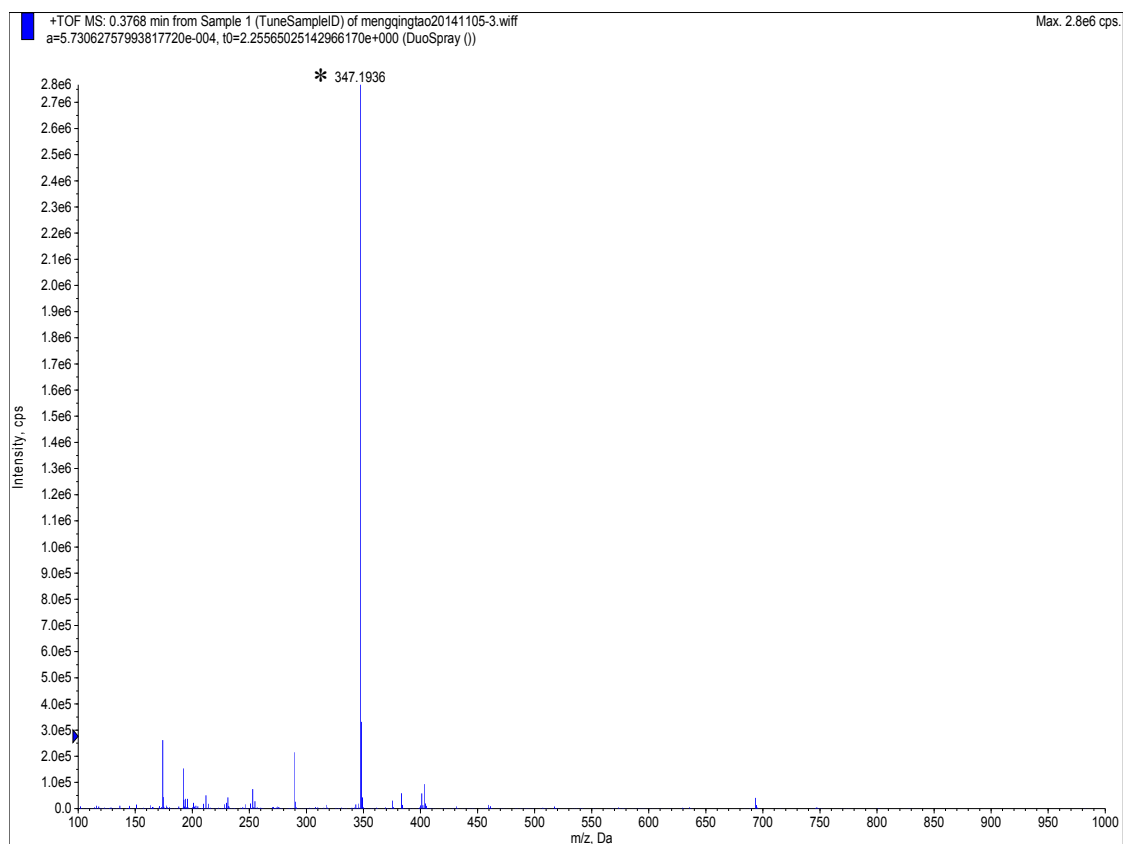


Figure S4. High resolution MS spectrum of 1,4,7-tris(carboxymethyl)-1,4,7,10-tetraazacyclododecane (DO3A).

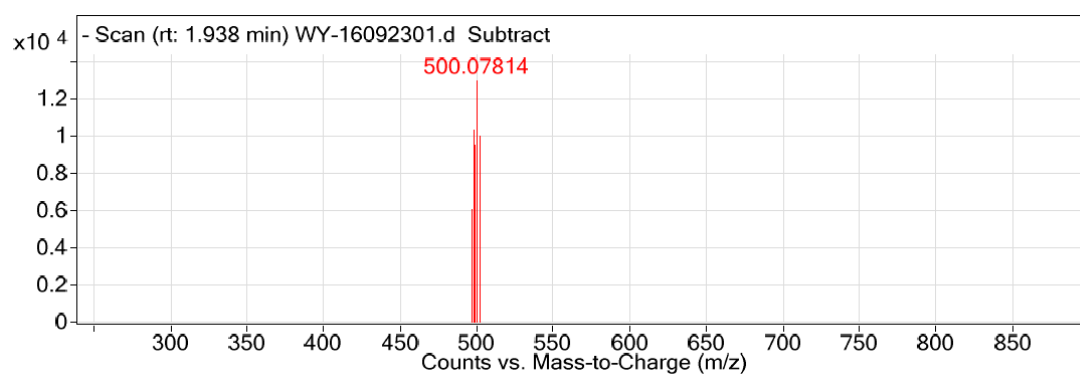


Figure S5. High resolution MS spectrum of [DO3A-Gd]⁻.

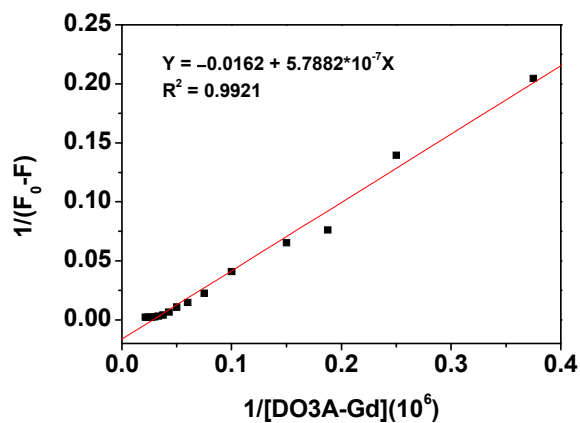


Figure S6. Benesi-Hildebrand plot (emission at 460 nm) of CA (10 μM) based on 1:1 binding stoichiometry with $[\text{DO3A-Gd}]^-$. Excitation was performed at 408 nm.

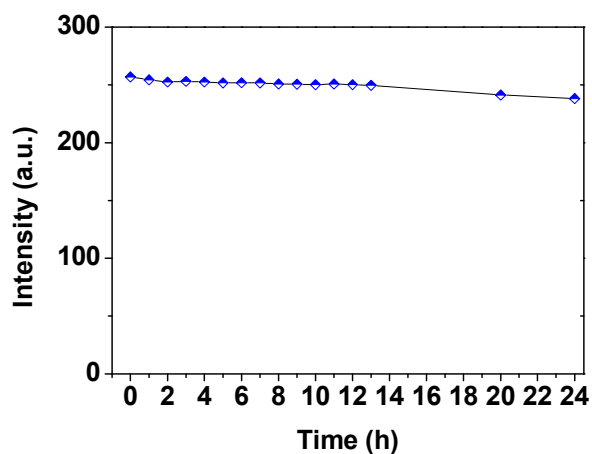


Figure S7. Fluorescence spectra of DO3A-Gd-CA (10 μM) at different times in $\text{CH}_3\text{CN-H}_2\text{O}$ (9:1, v/v , pH = 7.4). The intensities were recorded at 460 nm, excitation at 408 nm.

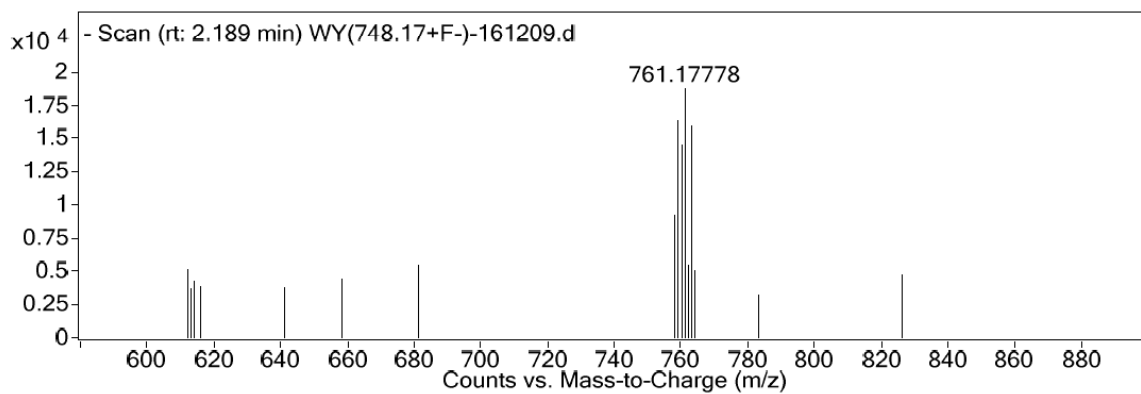


Figure S8. High resolution MS spectrum of $[\text{DO3A-Gd-CA}]^-$.

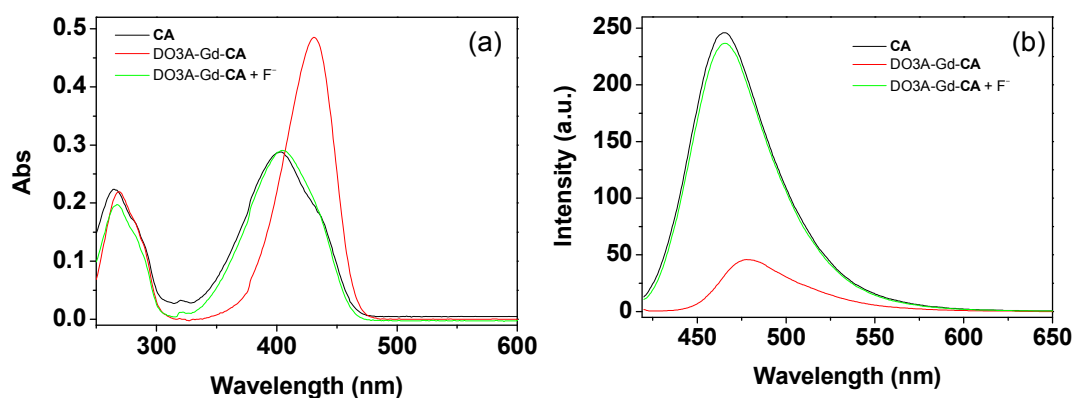


Figure S9. UV-vis absorption (a) and emission spectra (b) of CA (10 μM) sequential upon addition of [DO3A-Gd]Na (15 μM) and fluoride ion (200 μM) in aqueous ($\text{CH}_3\text{CN}:\text{H}_2\text{O} = 9:1$, $\text{pH} = 7.4$).

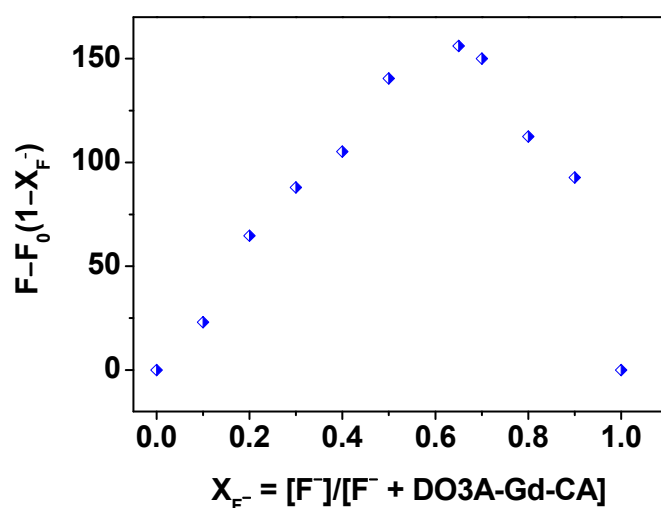


Figure S10. Job's plot of DO3A-Gd-CA toward fluoride ions in aqueous ($\text{CH}_3\text{CN}:\text{H}_2\text{O} = 9:1$, $\text{pH} = 7.4$).

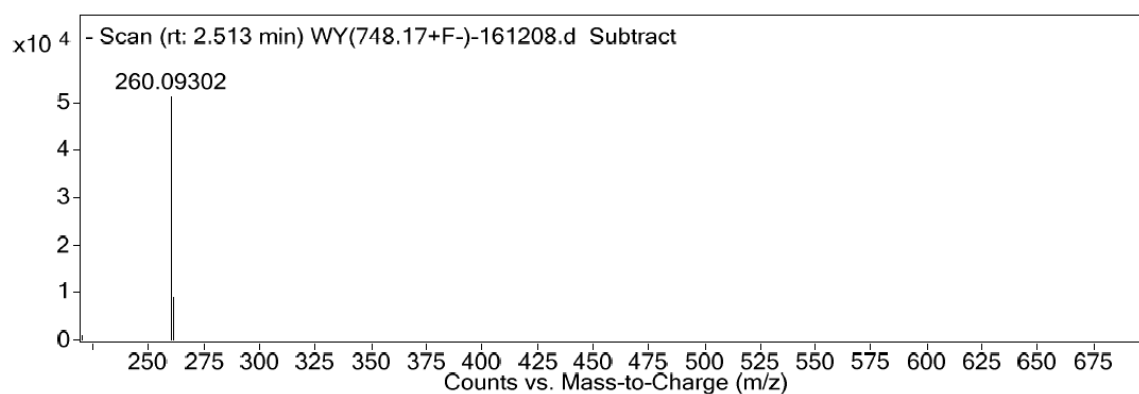


Figure S11. High resolution MS spectrum of DO3A-Gd-CA in presence of fluoride ions in aqueous.

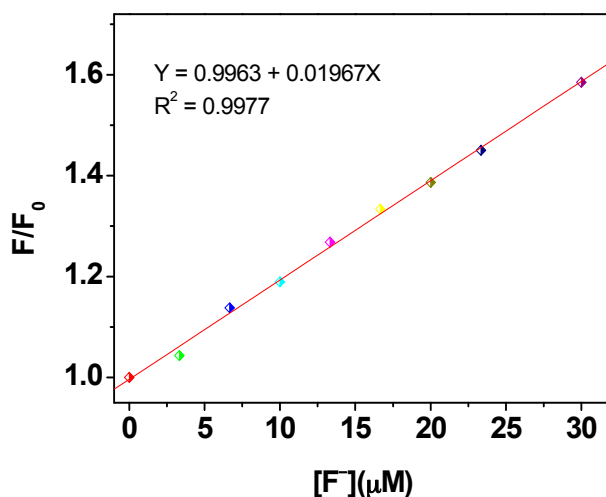


Figure S12. Linear relationship between fluorescence intensity of DO3A-Gd-CA (5 μM) at 460 nm versus the concentration of fluoride ion (0–30 μM) in aqueous (CH₃CN:H₂O = 9:1). Excitation was performed at 408 nm.

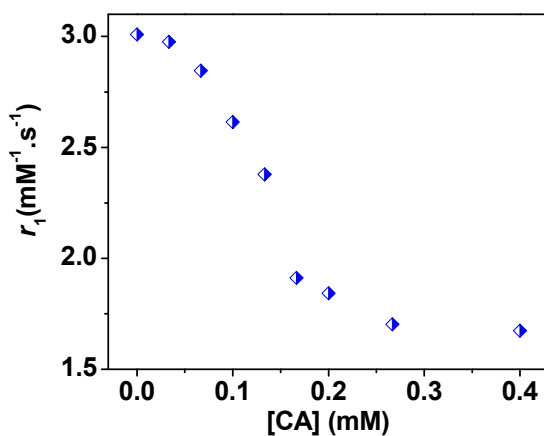


Figure S13. Changes in the longitudinal relaxivity (r_1) of DO3A-Gd (0.2 mM) as a function of the CA concentration (0–0.4 mM) in CH₃CN-H₂O (9:1, v/v, pH = 7.4).

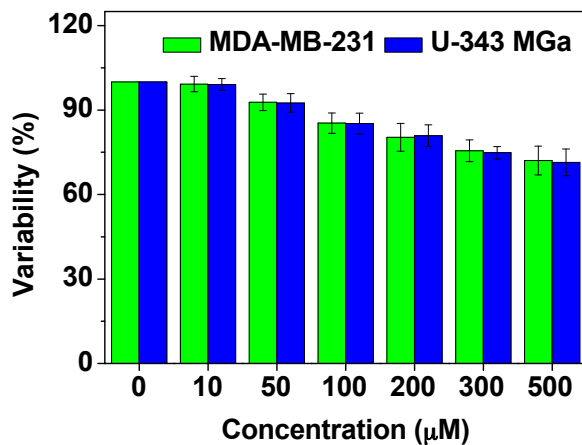


Figure S14. MDA-MB-231 and U-343 MGa cell viability values (%) assessed using an MTT proliferation test versus incubation concentrations of DO3A-Gd-CA.

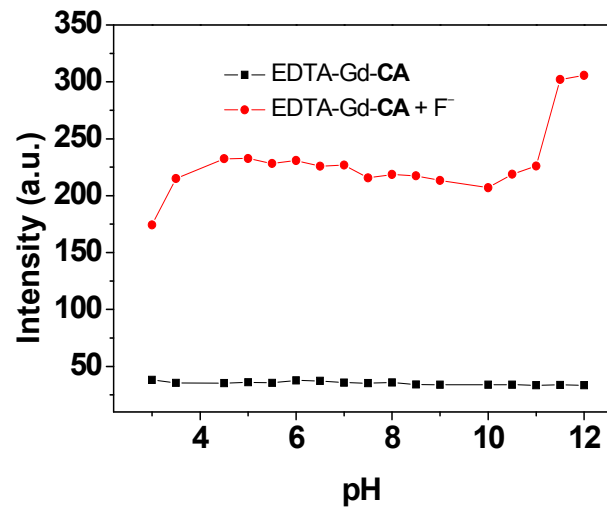


Figure S15. Influence of pH on the fluorescence intensities of DO3A-Gd-CA in the absence and presence of fluoride ion. The intensities were recorded at 460 nm, excitation was performed at 408 nm.

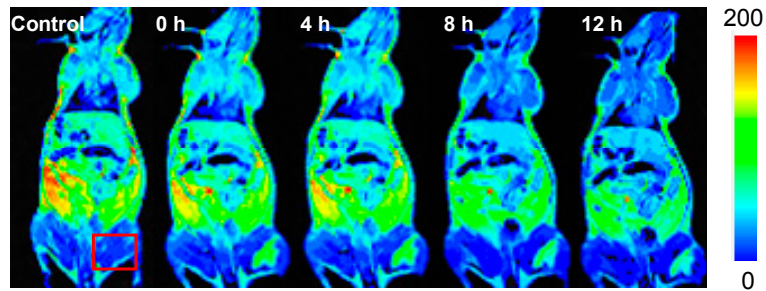


Figure S16. In vivo T₁-weighted MR pseudocolor images of mice at four representative time points after subcutaneous injection of DO3A-Gd-CA into one hind leg of mouse (0.2 mL, 0.2 mM).